



The Journal of
NUCLEAR MEDICINE

Synthesis and Preliminary Evaluation of ^{18}F -Labeled Pyridaben Analogues for Myocardial Perfusion Imaging with PET

Tiantian Mou, Zuoquan Zhao, Wei Fang, Cheng Peng, Feng Guo, Boli Liu, Yunchuan Ma and Xianzhong Zhang

J Nucl Med. 2012;53:472-479.

Published online: February 2, 2012.

Doi: 10.2967/jnumed.111.088096

This article and updated information are available at:

<http://jnm.snmjournals.org/content/53/3/472>

Information about reproducing figures, tables, or other portions of this article can be found online at:


<http://jnm.snmjournals.org/site/misc/permission.xhtml>

Information about subscriptions to JNM can be found at:

<http://jnm.snmjournals.org/site/subscriptions/online.xhtml>

The Journal of Nuclear Medicine is published monthly.
SNMMI | Society of Nuclear Medicine and Molecular Imaging
1850 Samuel Morse Drive, Reston, VA 20190.
(Print ISSN: 0161-5505, Online ISSN: 2159-662X)

© Copyright 2012 SNMMI; all rights reserved.

 SOCIETY OF
NUCLEAR MEDICINE
AND MOLECULAR IMAGING

Synthesis and Preliminary Evaluation of ^{18}F -Labeled Pyridaben Analogues for Myocardial Perfusion Imaging with PET

Tiantian Mou¹, Zuoquan Zhao¹, Wei Fang², Cheng Peng³, Feng Guo², Boli Liu¹, Yunchuan Ma³, and Xianzhong Zhang¹

¹Key Laboratory of Radiopharmaceuticals, Ministry of Education, College of Chemistry, Beijing Normal University, Beijing, China;

²Department of Nuclear Medicine, Cardiovascular Institute and Fu Wai Hospital, Chinese Academy of Medical Sciences, Beijing, China; and ³PET Center of Xuan Wu Hospital, Capital Medical University, Beijing, China

In this study the ^{18}F -labeled pyridaben analogs 2-tert-butyl-4-chloro-5-(4-(2- ^{18}F -fluoroethoxy))benzyloxy-2H-pyridazin-3-one (^{18}F -FP1OP) and 2-tert-butyl-4-chloro-5-(4-(2-(2-(2- ^{18}F -fluoroethoxy)ethoxy)ethoxy))benzyloxy-2H-pyridazin-3-one (^{18}F -FP3OP) were synthesized, characterized, and evaluated as potential myocardial perfusion imaging (MPI) agents with PET. **Methods:** The tosylate labeling precursors of 2-tert-butyl-4-chloro-5-(4-(2-tosyloxy-ethoxy))benzyloxy-2H-pyridazin-3-one (OTs-P1OP), 2-tert-butyl-4-chloro-5-(4-(2-(2-(2-tosyloxy-ethoxy)ethoxy)ethoxy))benzyloxy-2H-pyridazin-3-one (OTs-P3OP), and the corresponding nonradioactive compounds (^{19}F -FP1OP and ^{19}F -FP3OP) were synthesized and characterized by infrared, ^1H nuclear magnetic resonance, ^{13}C nuclear magnetic resonance, and mass spectrometry analysis. ^{18}F -FP1OP and ^{18}F -FP3OP were obtained by 1-step nucleophilic substitution of tosyl with ^{18}F and evaluated as MPI agents in vitro (physicochemical properties, stability), ex vivo (autoradiography), and in vivo (toxicity and biodistribution in normal mice; cardiac PET in healthy Chinese mini swine and in acute myocardial infarction and chronic myocardial ischemia models). **Results:** The total radiosynthesis time of both tracers, including final high-pressure liquid chromatography purification, was about 70–90 min. Typical decay-corrected radiochemical yields were about 50%, and the radiochemical purities were more than 98% after purification. ^{18}F -FP1OP had lower hydrophilicity and higher water stability than that of ^{18}F -FP3OP. In biodistribution studies, both ^{18}F -FP1OP and ^{18}F -FP3OP had high heart uptake (31.13 ± 6.24 and 31.10 ± 3.72 percentage injected dose per gram at 2 min after injection, respectively) and high heart-to-liver, heart-to-lung, and heart-to-blood ratios at all time points after injection. Further autoradiography evaluation of ^{18}F -FP1OP showed that the heart uptake could be blocked effectively by rotenone or nonradioactive ^{19}F -FP1OP. Clear cardiac PET images of ^{18}F -FP1OP were obtained in healthy Chinese mini swine at 2, 15, 30, 60, and 120 min after injection, and the uptake of perfusion deficit

areas was much lower than in normal tissue in both acute myocardial infarction and chronic myocardial ischemia models. **Conclusion:** The ^{18}F -labeled pyridaben analogs reported in this study have high heart uptake and low background uptake in both the mouse model and the Chinese mini swine model. The tracer with the shorter radiolabeling side chain (^{18}F -FP1OP) has better stability, faster clearance from the major organs, and a higher heart-to-liver ratio than the other tracer (^{18}F -FP3OP). On the basis of the promising biologic properties, this mitochondrial complex I-targeted tracer (^{18}F -FP1OP) is worthy to be developed as an MPI agent and to be compared with the other PET MPI agents in the future.

Key Words: MPI; MC-I; ^{18}F ; animal imaging; radiopharmaceuticals

J Nucl Med 2012; 53:472–479

DOI: 10.2967/jnumed.111.088096

Myocardial perfusion imaging (MPI) is a significant method of noninvasive measurement in the diagnosis and prognosis of coronary artery disease. Though $^{99\text{m}}\text{Tc}$ -sestamibi has been the gold standard of MPI for decades in nuclear medicine (1), it still has several weaknesses compared with PET (2). Currently, since ^{18}F has an appropriate physical half-life, good biocompatibility, a suitable atomic radius, and high resolution with PET technology (3), some ^{18}F -labeled lipophilic cations (such as ^{18}F -TPP (4,5), ^{18}F -FBnTP (1,6), and ^{18}F -FERhB (7)) and analogs of mitochondrial complex I (MC-I) inhibitors (such as ^{18}F -FDHR (8), ^{18}F -RP1003/04/05 (9), and 2-tert-butyl-4-chloro-5-[4-(2- ^{18}F -fluoroethoxymethyl)benzyloxy]-2H-pyridazin-3-one (BMS-747158-02) (10)) have been reported as potential MPI agents. Most of those compounds have better image quality and a better relationship to true myocardial blood flow than $^{99\text{m}}\text{Tc}$ -sestamibi (11,12). Up to now, BMS-747158-02 (also known by the nonproprietary name *flurpiridaz*) has been the best evaluated ^{18}F -labeled MPI agent. It has high (94%) first-pass extraction fraction (12), its high myocardial uptake is proportional to myocardial blood flow, and it has entered clinical development (phase 3) (11). The promising properties of BMS-

Received Aug. 7, 2011; revision accepted Oct. 5, 2011.

For correspondence or reprints contact any of the following: Xianzhong Zhang, College of Chemistry, Beijing Normal University, 19 Xijiekou Outer St., Beijing 100875, China.

E-mail: zhangxzh@gmail.com

Boli Liu, College of Chemistry, Beijing Normal University, 19 Xijiekou Outer St., Beijing 100875, China.

E-mail: liuboli@bnu.edu.cn

Wei Fang, Department of Nuclear Medicine, Cardiovascular Institute and Fu Wai Hospital, Chinese Academy of Medical Sciences, Beijing 100037, China.

E-mail: tsenyuan@yahoo.com.cn

Published online Feb. 2, 2012.

COPYRIGHT © 2012 by the Society of Nuclear Medicine, Inc.

747158-02 will ensure that cardiac PET will be the standard for evaluation of myocardial perfusion in coming years.

Currently, clinical use of approved PET agents for MPI is limited by the inherent properties of radioisotopes, the degree of flow alteration, or the requirement for an on-site cyclotron. The development of an ideal ^{18}F -labeled myocardial perfusion tracer that can be produced and widely distributed by a central cyclotron facility remains a challenge. Mitochondria take up about 20%–30% of the myocardial intracellular volume in the heart (13). Therefore, the development of mitochondrion-targeted ^{18}F -labeled analogs of MC-I inhibitors as potential MPI agents is of great interest. Several classes of MC-I inhibitors have been reported, such as fenazaquin, *S*-chromone, tebufenpyrad, and pyridaben; all have the same binding site of the MC-I enzyme as rotenone (14,15). Our laboratories have been particularly interested in analogs of pyridaben. Recently, we reported a pyridaben analog 2-tert-butyl-5-[4-(2-(^{18}F -fluoroethoxy)ethoxy)benzyloxy]-4-chloro-2H-pyridazin-3-one (^{18}F -FP2OP) as a potential MPI agent with promising properties (16). It has high heart uptake and good heart-to-nontarget ratios. However, ^{18}F -FP2OP is not very stable in water, obviously limiting its application. Accordingly, 2 new tracers with different lengths of radiolabeling side chain were developed to improve stability while retaining the promising properties. Herein, we report the synthesis and evaluation of 2-tertbutyl-4-chloro-5-(4-(2-(^{18}F -fluoroethoxy)benzyloxy)-2H-pyridazin-3-one (^{18}F -FP1OP) and 2-tertbutyl-4-chloro-5-(4-(2-(2-(^{18}F -fluoroethoxy)ethoxy)ethoxy)benzyloxy)-2H-pyridazin-3-one (^{18}F -FP3OP) as potential MPI agents.

MATERIALS AND METHODS

Materials

$^{18}\text{F}\text{-F}^-$ was obtained from the PET Center of Xuanwu Hospital. No-carrier-added $^{18}\text{F}\text{-F}^-$ was trapped on a QMA cartridge (Waters) and eluted with 0.3 mL of K_2CO_3 solution (10 mg/mL in H_2O) combined with 1 mL of Kryptofix 2.2.2. solution (Sigma-Aldrich) (13 mg/mL in acetonitrile) (17,18). Rotenone with 95% purity was purchased from Sigma-Aldrich. Other reagents and solvents were purchased from commercial suppliers. Paper electrophoresis experiments were performed using 0.025 M phosphate buffer (pH 7.4) and #1 filter paper (Xinhua) at 150 V for 180 min. Reversed-phase high-pressure liquid chromatography (HPLC) was performed on a system with an LC-20AT pump (Shimadzu) and a B-FC-320 flow counter (Bioscan). The C-18 reverse-phase semipreparative HPLC column (10 × 250 mm, 5- μm particle size [Venusil MP-C18; Agela Technologies Inc.]) was eluted at a flow rate of 5 mL/min. A Labgen 7 homogenizer was used (Cole-Parmer Instruments). ^1H nuclear magnetic resonance spectra were recorded on a 400-MHz spectrometer (Bruker), and ^{13}C nuclear magnetic resonance spectra were recorded on a 100-MHz spectrometer (Bruker). Chemical shifts are reported in δ (ppm) values. Infrared spectra were measured on a Nicolet 360 Avatar instrument (Thermo) using a potassium bromide disk, scanning from 400 to 4,000 cm^{-1} . Mass spectra were recorded using an Apex IV FTM instrument (Bruker).

Kunming mice (18–20 g) were obtained from the Animal Center of Peking University. Healthy Chinese mini swine and cardiac ischemia models (about 15 kg) were obtained from the Animal Center of Fu Wai

Hospital. All biodistribution studies were performed under a protocol approved by Beijing Administration Office of Laboratory Animals.

Chemistry

As shown in Supplemental Figure 1 (supplemental materials are available online only at <http://jnm.snmjournals.org>), the tosylate precursors of 2-tert-butyl-4-chloro-5-(4-(2-tosyloxy-ethoxy))-benzyloxy-2H-pyridazin-3-one (OTs-P1OP), 2-tert-butyl-4-chloro-5-(4-(2-(2-(2-tosyloxy-ethoxy)ethoxy)ethoxy))-benzyloxy-2H-pyridazin-3-one (OTs-P3OP), and the corresponding nonradioactive reference compounds (^{19}F -FP1OP and ^{19}F -FP3OP) were synthesized and characterized according to a procedure published previously (14,16). Details of the synthesis and the characterization data are available in the online supplemental data.

Radiochemistry

The labeling procedure of ^{18}F -FP1OP and ^{18}F -FP3OP, shown in Figure 1, is similar to that we published previously, with slight modification (16). Briefly, after the solvent of the $^{18}\text{F}\text{-F}^-$ eluate was evaporated under a stream of nitrogen at 110°C, 1.5 mg of tosylate precursor dissolved in anhydrous acetonitrile (1.5 mg/mL) were added. After 30 min of stirring at 90°C and then cooling to room temperature, the reaction mixture was injected onto a semi-HPLC column for purification. The column was eluted with water (solvent A) and acetonitrile (solvent B) at a flow rate of 5.0 mL/min. The gradient was 95% A from 0 to 5 min, 95%–60% A from 5.01 to 8 min, 60%–35% A from 8.01 to 19 min, and 0% A from 19.01 to 30 min. The desired product was collected from the HPLC column, and the solvent was evaporated using a rotary evaporator. The product was redissolved in 5% ethanol solution and filtered through a 0.22- μm Millipore filter.

The final radiochemical purity was determined by reinjection of the product onto a radio-HPLC column, and the radioactive fraction was collected and measured in a dose calibrator for specific activity calculation. The mass of the product was calculated by comparing the area under the ultraviolet curve at 254 nm with that of the standard reference (Supplemental Fig. 2).

Physicochemical Properties Studies

A previously published procedure (16,19) was used to measure the octanol-to-water partition coefficient and to perform the paper electrophoresis experiment. The partition coefficient value, expressed as log *P*, was measured in 1-octanol and phosphate buffer (0.025 M, pH 7.4). For paper electrophoresis experiments, after development in phosphate buffer (0.025 M, pH 7.4) the radioactivity distribution on the strip was determined using a 1470 Wizard automatic γ -counter (Perkin-Elmer).

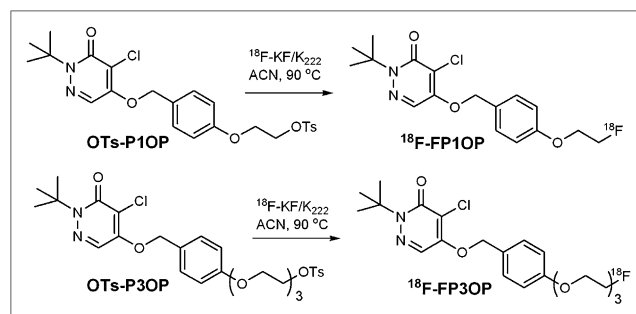


FIGURE 1. Radiolabeling route of ^{18}F -FP1OP and ^{18}F -FP3OP. ACN = acetonitrile; K_{222} = Kryptofix 2.2.2.; KF = potassium fluoride.

In vitro stability was tested by following a published procedure (16,20). Briefly, the radiotracer was incubated in water at room temperature for 1 h, in 80% ethanol solution at room temperature for 4 h, and in 0.5 mL of murine plasma at 37°C for 1 h. Plasma proteins were precipitated by adding 100 μ L of acetonitrile and were removed by centrifugation. Afterward, the radiochemical purity was again assayed by HPLC.

Biodistribution Study

About 185 kBq of radiotracer (^{18}F -FP1OP or ^{18}F -FP3OP) in 0.1 mL of 5% ethanol solution were injected through the tail vein of normal Kunming mice ($n = 5$). The mice were sacrificed at 2, 15, 30, and 60 min after injection, and the tissues and organs of interest were collected, weighed wet, and counted in a γ -counter. The percentage of injected dose per gram (%ID/g) for each sample was calculated by comparing its activity with an appropriate standard of injected dose. The values were expressed as mean \pm SD.

Metabolic Stability

Normal Kunming mice were intravenously injected with 3.7 MBq of the ^{18}F -FP1OP solution. The animals were sacrificed and dissected at 2 and 30 min after injection. Blood, urine, and heart were collected and treated using a previously published procedure (16,21). Briefly, the blood sample was immediately centrifuged for 5 min at 13,200 rpm. The heart was homogenized and suspended in 1 mL of methanol and then centrifuged for 5 min at 13,000 rpm. The urine sample was directly diluted with 1 mL of phosphate-buffered saline (0.025 M, pH 7.4). The heart and blood supernatants and diluted urine samples were collected and passed through a Sep-Pak C18 cartridge (Waters). All cartridges were washed with 0.5 mL of water and eluted with 0.5 mL of methanol. The combined aqueous and organic solutions were passed through a 0.22- μ m filter (Millipore) and analyzed by radio-HPLC using the procedure described above.

Toxicity Study

Normal Kunming mice were fed a standard diet for 48 h before treatment. They then were kept fasting overnight (12 h) and weighed before treatment (22). A group of 5 male and 5 female mice was treated with each dose level of nonradioactive ^{19}F -FP1OP (1.0142, 1.1064, 1.2171, 1.3830, and 1.6043 mg/kg) or saline through tail vein injection. The mice were observed for 7 d after injection, and mortality was recorded.

Ex Vivo Autoradiography

Heart slides were obtained from a normal Sprague Dawley rat (Harlan Laboratories, Inc.) (16). After being dehydrated with 30% sucrose solution at 4°C, the heart was sectioned (30 μ m) with a cryostat (CM1900; Leica) and thaw-mounted onto Superfrost microscope slides (Erie Scientific Co.). Frozen sections were fixed in acetone and air-dried at room temperature before use. The slides were pretreated with 100 μ L of saline, 20 μ M rotenone, or 20 μ M ^{19}F -FP1OP solution at room temperature for 30 min. After removal of that solution, 100 μ L of ^{18}F -FP1OP solution (about 14 kBq) were added to the sections and incubated at room temperature for another 30 min. After being washed with water and 40% ethanol solution, the sections were subjected to autoradiography for 10 min. Images were developed and quantified in a Cyclone Phosphorimager system (Perkin-Elmer Inc.).

Whole-Body PET/CT of Healthy Animal

Animal procedures were performed following National Institutes of Health guidelines and were approved by Fu Wai Hospital, Chinese Academy of Medical Science.

For the whole-body PET/CT study, a healthy Chinese mini swine was anesthetized by a mixture of ketamine (25 mg/kg) and diazepam (1.1 mg/kg). Anesthesia was supplemented as needed. The animal was placed prone on the PET/CT bed, and a venous catheter was established for radiotracer injection. About 55 MBq of ^{18}F -FP1OP in 2 mL of 5% ethanol solution were injected intravenously.

Whole-body imaging was performed at 2, 15, 30, 60, and 120 min after injection. PET data were acquired on a PET/CT system (Biograph 64; Siemens Healthcare). Whole-body scanning involved 4 bed positions, with each scanned for 2 min. Regions of interest were drawn on the myocardium, liver, and lung. Standardized uptake value was calculated as [mean region-of-interest count (cps/pixel) \times body weight (kg)]/[injected dose (mCi) \times calibration factor (cps/pixel)]. The myocardium-to-liver and myocardium-to-lung standardized uptake value ratios at each time point were evaluated.

Cardiac PET/CT Scans of Disease Models

For the model of acute myocardial infarction, a Chinese mini swine was anesthetized with intravenous injection of sodium pentobarbital (25–35 mg/kg), and additional sodium pentobarbital was used via intravenous injection to maintain anesthesia, when needed. Heart rate and electrocardiography were recorded throughout. The animal underwent lateral thoracotomy at the level of the fifth left intercostal space, and the heart was suspended in a pericardial cradle. The left anterior descending coronary artery was isolated to the section about 1.5 cm after the first major diagonal branch. A silk suture was placed around the artery and ligated to block the coronary flow. Acute myocardial infarction induced by ligation was conformed by electrocardiography. A dose of about 55 MBq of ^{18}F -FP1OP was injected at 60 min after the thoracic incision had been closed.

The chronic myocardial ischemia model was created in a Chinese mini swine by ligation of the left anterior descending coronary artery at about 1.5 cm after the first major diagonal branch, using an amaroid constrictor, to produce progressive vessel occlusion and ischemia. Three weeks later, when a critical stenosis (>80%) was confirmed by coronary angiography (Supplemental Fig. 3), a dose of about 55 MBq of ^{18}F -FP1OP was injected before cardiac PET/CT.

The cardiac PET scans were performed at 2, 15, 30, 60, and 120 min after injection. After a low-dose CT scan for attenuation correction (tube voltage, 120 kV; tube current, 50 mAs with CareDose4D technique (Siemens); collimation, 24×1.2 mm; rotation time, 0.5 s; pitch, 1.2; slice width, 3 mm), PET was performed to evaluate myocardial uptake. Using list mode with electrocardiography gating, the scan time was 10 min. The images were reconstructed with iterative ordered-subsets expectation maximization (2 iterations and 8 subsets). The matrix size was 2.0×2.0 mm with 128×128 pixels, and the slice thickness was 3.125 mm.

RESULTS

Chemistry

The precursors (OTs-P1OP and OTs-P3OP) and the corresponding nonradioactive references (^{19}F -FP1OP and ^{19}F -FP3OP) were synthesized and characterized by ^1H , ^{13}C , and ^{19}F nuclear magnetic resonance; electrospray ionization–mass spectrometry; infrared analysis; and elemental analysis. The synthesis route and all analysis data are shown in Supplemental Figure 1.

As shown in Figure 2, HPLC analysis of ^{19}F -FP1OP and ^{19}F -FP3OP showed that their retention times were 22.0 and 20.3 min, respectively (Figs. 2A and 2C). The delayed retention time of ^{19}F -FP1OP indicated that the compound with the shorter radiolabeling chain has lower polarity and hydrophilicity. Their chemical purity was calculated as more than 98% from the HPLC chromatogram ($\lambda = 254$ nm), suggesting they are acceptable reference standards for the corresponding radioactive tracers.

Radiochemistry

The radiolabeling route is shown in Figure 1. Starting from $^{18}\text{F}\text{-F}^-$ in a Kryptofix 2.2.2./ K_2CO_3 solution, the total reaction time, including final HPLC purification, was 70–90 min. The overall decay-corrected radiochemical yields were $58\% \pm 7.4\%$ and $47\% \pm 6.8\%$ for ^{18}F -FP1OP and ^{18}F -FP3OP, respectively. The radio-HPLC retention times of ^{18}F -FP1OP and ^{18}F -FP3OP were 22.3 and 20.9 min, respectively (Figs. 2B and 2D) and were highly consistent

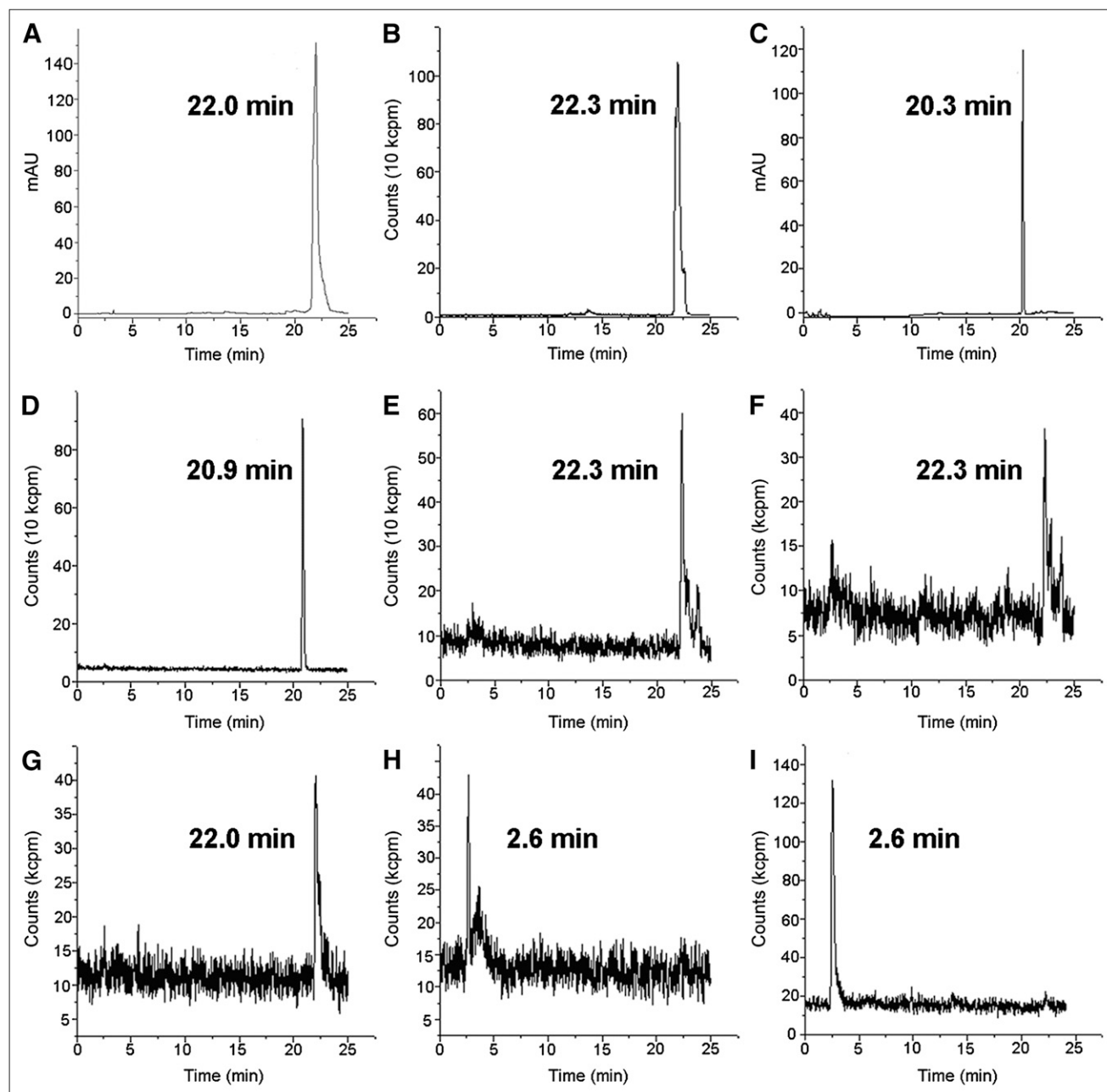


FIGURE 2. HPLC chromatograms of compounds ^{19}F -FP1OP (A), ^{18}F -FP1OP (B), ^{19}F -FP3OP (C), and ^{18}F -FP3OP (D) and profiles of metabolic stability study of ^{18}F -FP1OP (soluble fractions were collected in heart at 2 min [E], in blood at 2 min [F], in heart at 30 min [G], in blood at 30 min [H], and in urine at 30 min [I]). Nonradioactive compounds of ^{19}F -FP1OP and ^{19}F -FP3OP were measured with ultraviolet detector, and radioactive compounds were measured radiometrically.

TABLE 1
Biodistribution Results of ^{18}F -FP1OP and ^{18}F -FP3OP in Normal Mice

Tissue	Compound	Postinjection time (min)			
		2	15	30	60
Heart	^{18}F -FP1OP	31.13 \pm 6.24	29.00 \pm 1.49	19.25 \pm 1.67	11.32 \pm 1.01
	^{18}F -FP3OP	31.10 \pm 3.72	33.52 \pm 5.03	29.85 \pm 3.89	22.06 \pm 3.91
Liver	^{18}F -FP1OP	2.72 \pm 0.33	1.86 \pm 0.14	1.77 \pm 0.20	2.14 \pm 0.29
	^{18}F -FP3OP	2.71 \pm 0.93	6.83 \pm 0.84	6.97 \pm 0.91	6.77 \pm 0.55
Spleen	^{18}F -FP1OP	3.45 \pm 0.98	2.49 \pm 0.49	2.41 \pm 0.22	2.34 \pm 0.17
	^{18}F -FP3OP	1.41 \pm 0.44	2.69 \pm 0.28	2.79 \pm 0.45	2.45 \pm 0.21
Lung	^{18}F -FP1OP	2.98 \pm 0.28	2.92 \pm 0.42	2.53 \pm 0.20	2.49 \pm 0.37
	^{18}F -FP3OP	4.65 \pm 1.60	1.58 \pm 0.33	1.78 \pm 0.51	1.90 \pm 0.26
Muscle	^{18}F -FP1OP	7.45 \pm 1.38	9.56 \pm 2.21	7.27 \pm 0.66	6.06 \pm 1.53
	^{18}F -FP3OP	5.55 \pm 2.51	6.96 \pm 0.86	7.87 \pm 0.58	6.85 \pm 0.86
Bone	^{18}F -FP1OP	2.23 \pm 0.22	3.56 \pm 0.53	4.13 \pm 0.54	5.28 \pm 2.29
	^{18}F -FP3OP	1.04 \pm 0.29	1.76 \pm 0.32	2.19 \pm 0.30	2.34 \pm 0.61
Kidney	^{18}F -FP1OP	23.69 \pm 3.16	16.31 \pm 2.76	10.50 \pm 0.75	6.63 \pm 0.68
	^{18}F -FP3OP	18.94 \pm 4.89	17.19 \pm 3.04	15.48 \pm 1.99	12.60 \pm 1.56
Blood	^{18}F -FP1OP	1.06 \pm 0.07	1.60 \pm 0.18	2.12 \pm 0.18	2.51 \pm 0.33
	^{18}F -FP3OP	0.82 \pm 0.05	0.69 \pm 0.10	0.89 \pm 0.16	1.07 \pm 0.12
Heart/liver	^{18}F -FP1OP	12.53	16.12	10.87	5.29
	^{18}F -FP3OP	11.48	4.91	4.28	3.26
Heart/lung	^{18}F -FP1OP	8.58	9.99	7.62	4.55
	^{18}F -FP3OP	6.69	21.28	16.75	11.61
Heart/blood	^{18}F -FP1OP	32.36	16.63	9.09	4.50
	^{18}F -FP3OP	37.9	48.77	33.57	20.61

Data are %ID/g \pm SD ($n = 5$).

with the corresponding nonradioactive references (Figs. 2A and 2C). The radiochemical purities calculated from radio-HPLC chromatograms of both tracers were more than 98% after purification. The specific activities of both tracers were estimated by HPLC analysis to be about 30 GBq/ μmol .

Physicochemical Properties

According to the results of the octanol-to-water partition coefficient and paper electrophoresis, ^{18}F -FP1OP and ^{18}F -FP3OP are lipophilic and neutral compounds. Their partition coefficients (log P) were 3.07 ± 0.13 and 1.25 ± 0.00 ($n = 3$), respectively. The shorter radiolabeling chain of ^{18}F -FP1OP leads to higher lipophilicity. This result is consistent with that of HPLC analysis.

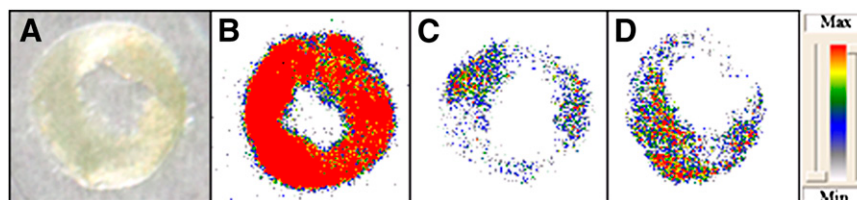
The HPLC profiles of stability studies are shown in Supplemental Figure 4. After storage in water at room temperature for 1 h, about 85% intact product of ^{18}F -FP1OP and 24% intact product of ^{18}F -FP3OP were eluted from HPLC. For the radiotracer incubated in murine plasma

at 37°C for 1 h, about 80% of ^{18}F -FP1OP was intact. When stocked in 80% ethanol solution, the tracers are stable during at least a 4-h period (Supplemental Fig. 4). Therefore, the HPLC-purified tracers are best stocked in 80% ethanol solution first. The stability studies show that the longer radiolabeling chain leads to worse stability in water (after storage in water for 1 h, about 85% of ^{18}F -FP1OP, 78% of ^{18}F -FP2OP, and 24% of ^{18}F -FP3OP are stable). Therefore, in the studies performed afterward, the most stable ^{18}F -FP1OP was selected for further evaluation.

Biodistribution in Mice

The biologic distribution results in mice are shown in Table 1. Both ^{18}F -FP1OP and ^{18}F -FP3OP had high initial heart uptake (31.13 ± 6.24 and 31.10 ± 3.72 %ID/g at 2 min after injection, respectively). Meanwhile, uptake in most other tissues was low, especially in liver and lung, resulting in the high heart-to-nontarget ratios for both tracers. For ^{18}F -FP1OP, the heart-to-liver, heart-to-lung, and

FIGURE 3. Autoradiograms of heart sections from normal Sprague Dawley rat (A is photograph of heart section before autoradiography). Sections were incubated with 100 μL of ^{18}F -FP1OP solution (about 14 kBq) for 30 min at room temperature after pretreatment with 100 μL of saline (B), 20 μM rotenone (C), or 20 μM ^{19}F -FP1OP (D).



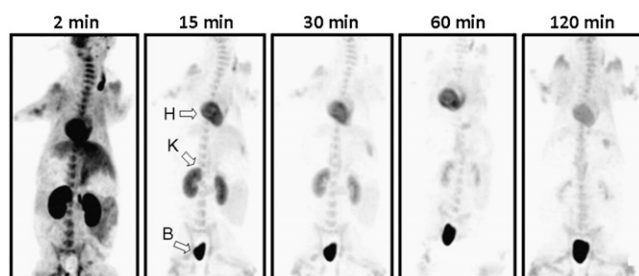


FIGURE 4. Whole-body planar images of healthy Chinese mini swine. Images were obtained with 55 MBq of ^{18}F -FP1OP in 5% ethanol solution at 2, 15, 30, 60, and 120 min after injection. B = urinary bladder; H = heart; K = kidney.

heart-to-blood ratios were 16.12, 9.99, and 16.63, respectively, at 15 min after injection. For ^{18}F -FP3OP, the respective ratios were 4.91, 21.28, and 48.77.

As described in Table 1, ^{18}F -FP1OP had high initial heart uptake and cleared quickly; about 64% of the tracer was eliminated from myocardium during the first hour after injection (11.32 ± 1.01 %ID/g at 60 min after injection). Compared with ^{18}F -FP1OP, ^{18}F -FP3OP had much slower clearance from myocardium, obviously higher liver uptake, and lower lung uptake at 2 min after injection, leading to the lower heart-to-liver and higher heart-to-lung ratios of ^{18}F -FP3OP than of ^{18}F -FP1OP. Both tracers had high initial kidney uptake, suggesting the tracers were excreted mainly via the renal system.

The reason for the slight increase of blood uptake of both tracers over time is not clear. The high uptake in muscle of both tracers may due to the high mitochondrial expression. All other organs and tissues had low uptake, and no obvious change was observed during the 60 min after injection.

Metabolic Stability

The metabolic stability of ^{18}F -FP1OP was determined in the heart, blood, and urine of Kunming mice at 2 and 30 min after injection. More than 95% of the total ^{18}F was eluted at 22.3 min from HPLC (Figs. 2E and 2F), suggesting that the

radioactivity in myocardium and blood at 2 min after injection was intact ^{18}F -FP1OP. At 30 min after injection, the tracer was still intact in myocardium (Fig. 2G) but was metabolized in blood and urine and eluted quickly from HPLC (Figs. 2H and 2I). The peak of ^{18}F -FP1OP had almost disappeared and a new metabolite appeared at about 2.6 min, suggesting the tracer undergoes considerable degradation in both blood and urine at 30 min after injection. No defluorination of ^{18}F -FP1OP was observed in vivo from HPLC analysis. This finding was confirmed by the low bone uptake found in the biodistribution study (Table 1).

Toxicity Study

Mortality data are shown in Supplemental Table 1. According to the Bliss method (23), the calculated lethal dose of 50% for the nonradioactive reference of ^{19}F -FP1OP was 1.2869 mg/kg (95% confidence limits, 1.1818–1.4015 mg/kg). On the basis of the toxicity result and the high specific activity (about 30 GBq/ μmol), this HPLC-purified tracer solution should be safe for injection.

Ex Vivo Autoradiography

Ex vivo autoradiography studies were performed on frozen sections of heart from a normal Sprague Dawley rat. As shown in Figure 3, ^{18}F -FP1OP had high uptake in myocardium (Fig. 3B) and could be blocked both by preincubation with rotenone (a known MC-I inhibitor with high affinity, Fig. 3C) and preincubation with ^{19}F -FP1OP (Fig. 3D). After calculation of the net radioactivity intensity, about 74% and 62% of the radioactivity were found to have been blocked by rotenone and ^{19}F -FP1OP, respectively. The results of autoradiography suggest that ^{19}F -FP1OP has the same binding site as, and comparable affinity to, rotenone. This is potent evidence that the ^{18}F -FP1OP was taken up by myocardium through the MC-I enzyme and remained in mitochondria.

Whole-Body PET/CT of Healthy Animal

The representative whole-body images of ^{18}F -FP1OP in a healthy Chinese mini swine are shown in Figure 4. The

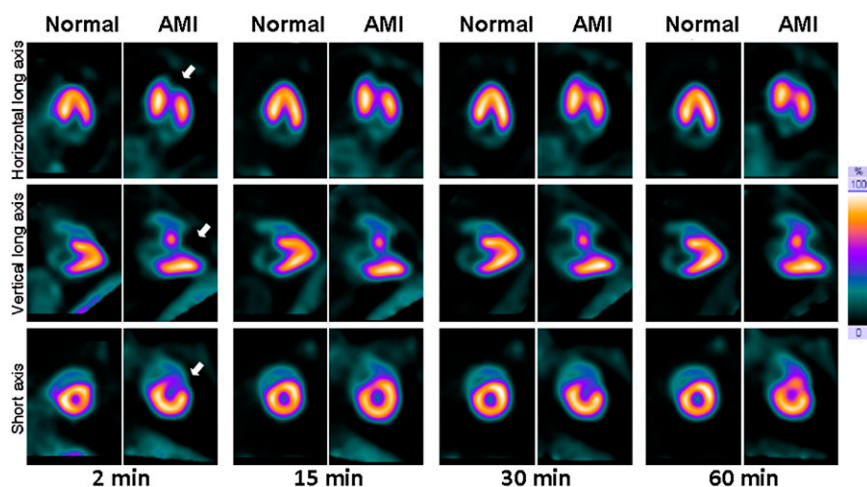


FIGURE 5. Cardiac PET images of healthy Chinese mini swine (normal) and Chinese mini swine with acute myocardial infarction (AMI). Images were obtained with 55 MBq of ^{18}F -FP1OP in 5% ethanol solution at 2, 15, 30, and 60 min after injection. Arrows indicate perfusion defect sites of infarction areas (apical and anterior walls).

heart could clearly be seen from 2 to 60 min after injection and was still visible at 120 min after injection, although heart uptake had obviously decreased. Radioactivity accumulated strongly in the kidney and cleared quickly to the bladder. Other organs and tissues had low background uptake. The heart-to-liver and heart-to-lung standardized uptake value ratios were, respectively, 1.83 and 4.53 at 2 min after injection, 2.33 and 6.25 at 15 min after injection, 2.73 and 7.39 at 30 min after injection, 3.03 and 8.77 at 60 min after injection, and 2.00 and 7.21 at 120 min after injection. The heart-to-liver and heart-to-lung ratios were highest at 60 min after injection, leading to a best PET acquisition time of 15–60 min after injection. In contrast, in the biodistribution study the highest heart-to-liver and heart-to-lung ratios were reached at only 15 min after injection; this difference may due to the different animal models used.

Cardiac PET/CT

The representative cardiac PET images of ^{18}F -FP1OP in healthy Chinese mini swine and the acute myocardial infarction model are shown in Figure 5. High heart activity was observed at all time points. Clearance agreed well with the biodistribution studies in mice. The outline of the myocardium was clear and uptake in background organs (liver and lung) low at all time points. In comparison with normal myocardium, the infarct region (apical and anterior wall) was apparent on ^{18}F -FP1OP cardiac PET in the acute myocardial infarction model (Fig. 5).

Representative cardiac PET images of the chronic myocardial ischemia model are shown in Figure 6. The perfusion deficit area (anterior wall) was clearly detected at 2–60 min after injection but showed a slightly redistribution of ^{18}F -FP1OP at 120 min after injection. Future experiments are needed to confirm the redistribution properties of ^{18}F -FP1OP.

DISCUSSION

Pyridaben possesses a hydrophobic heterocyclic headpiece, a side chain of *p*-tert-butylphenyl moiety, and a heteroatom-

containing linker (14). In this study, we found that the side chain had a significant impact on the stability and pharmacokinetic properties of pyridaben-based radiotracers. According to the physicochemical properties study, the compound with the shorter polyethylene glycol chain had higher lipophilicity and better stability. For example, ^{18}F -FP1OP, which had the shortest polyethylene glycol chain, displayed the highest lipophilicity and the best stability. Furthermore, changes of the radiolabeling chain could also affect biodistribution (Supplemental Fig. 5). The biodistribution comparison of ^{18}F -FP1OP, ^{18}F -FP2OP (16), and ^{18}F -FP3OP showed that ^{18}F -FP1OP had the lowest liver uptake and the fastest clearance rate from the liver (Supplemental Fig. 5). ^{18}F -FP1OP had the best stability, the highest heart-to-liver ratio at all time points, and acceptable heart-to-lung and heart-to-blood ratios—all promising properties making it superior to the other 2 tracers.

^{18}F -FP1OP had higher initial heart uptake and lower initial liver uptake than that of BMS-747158-02, making it possible to acquire PET data earlier after injection. This feature will be of great benefit to patients by shortening their waiting time significantly. In addition, ^{18}F -FP1OP cleared from myocardium much more quickly than did BMS-747158-02; this property could definitely lower the irradiation dose and make the tracer a good choice for stress and rest imaging in a 1-d protocol.

Because inhibiting MC-I activity might lead to death of the animal, ex vivo autoradiography was done instead to confirm the specific binding of ^{18}F -FP1OP to MC-I enzyme. The toxicity of the tracer as a pyridaben analog should be considered seriously. In this study, the 50% lethal dose of ^{19}F -FP1OP was determined in mice by tail vein injection as 1.2869 mg/kg. On the basis of the reported specific activity (about 30 GBq/ μmol), if 370 MBq of tracer were to be injected in a 70-kg human, the mass of ^{19}F -FP1OP would be about 4.37 μg , and the safety factor is calculated as more than 20,000 times the lethal dose of 50%. Therefore, we believe the radiotracer is safe enough for PET application. Acute or single-dose toxicity and other special safety studies will be done in the future.

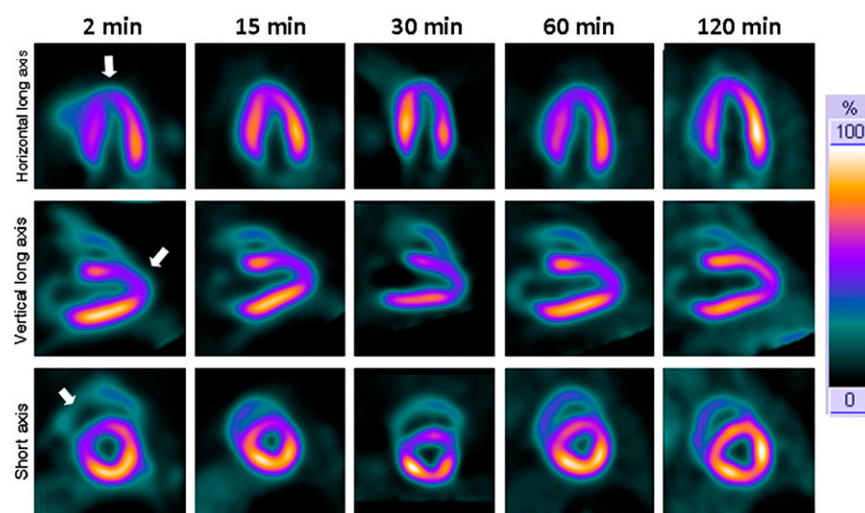


FIGURE 6. Cardiac PET images of Chinese mini swine with chronic myocardial ischemia. Images were obtained with 55 MBq of ^{18}F -FP1OP in 5% ethanol solution at 2, 15, 30, 60, and 120 min after injection. Arrows indicate sites of perfusion deficit regions (anterior wall). Redistribution was observed at 120 min after injection.

CONCLUSION

The 2 lipophilic and neutral tracers ^{18}F -FP1OP and ^{18}F -FP3OP were successfully prepared with high radiochemical yield ($\sim 50\%$) and radiochemical purity ($>98\%$). Both had high initial heart uptake and good heart-to-nontarget ratios. The better stability and faster clearance from myocardium of ^{18}F -FP1OP make it worthy to be evaluated as an MPI agent, and the high specific activity makes it a safe injection. The heart of a healthy Chinese mini swine could be imaged clearly at 2–60 min after injection by cardiac PET. The infarction region could be detected clearly in both acute myocardial infarction and chronic myocardial ischemia models of Chinese mini swine, suggesting the potential usefulness of ^{18}F -FP1OP as an MPI agent.

DISCLOSURE STATEMENT

The costs of publication of this article were defrayed in part by the payment of page charges. Therefore, and solely to indicate this fact, this article is hereby marked “advertisement” in accordance with 18 USC section 1734.

ACKNOWLEDGMENTS

We thank Huihui Jing, Wenjiang Yang, and Wenyan Guo for their generous help. This project was sponsored by the National Natural Science Foundation of China (20871020) and Beijing Natural Science Foundation (2092018) and supported partially by Fundamental Research Funds for the Central Universities and the Scientific Research Foundation for the Returned Overseas Chinese Scholars, State Education Ministry. No other potential conflict of interest relevant to this article was reported.

REFERENCES

1. Madar I, Ravert HT, Du Y, et al. Characterization of uptake of the new PET imaging compound ^{18}F -fluorobenzyl triphenyl phosphonium in dog myocardium. *J Nucl Med*. 2006;47:1359–1366.
2. Le Guludec D, Lautamäki R, Knuuti J, Bax J, Bengel F. Present and future of clinical cardiovascular PET imaging in Europe: a position statement by the European Council of Nuclear Cardiology (ECNC). *Eur J Nucl Med Mol Imaging*. 2008;35:1709–1724.
3. Kopka K, Schober O, Wagner S. ^{18}F -labelled cardiac PET tracers: selected probes for the molecular imaging of transporters, receptors and proteases. *Basic Res Cardiol*. 2008;103:131–143.
4. Cheng Z, Subbarayan M, Chen X, Gambhir SS. Synthesis of (4- ^{18}F fluorophenyl)triphenylphosphonium as a potential imaging agent for mitochondrial dysfunction. *J Labelled Comp Radiopharm*. 2005;48:131–137.
5. Shoup TM, Elmaleh D, Brownell A-L, Zhu A, Guerrero J, Fischman A. Evaluation of (4- ^{18}F fluorophenyl)triphenylphosphonium ion: a potential myocardial blood flow agent for PET. *Mol Imaging Biol*. 2011;13:511–517.
6. Ravert HT, Madar I, Dannals RF. Radiosynthesis of 3- ^{18}F fluoropropyl and 4- ^{18}F fluorobenzyl triarylphosphonium ions. *J Labelled Comp Radiopharm*. 2004;47:469–476.
7. Heinrich TK, Gottumukkala V, Snay E, et al. Synthesis of fluorine-18 labeled rhodamine B: a potential PET myocardial perfusion imaging agent. *Appl Radiat Isot*. 2010;68:96–100.
8. Marshall RC, Powers-Risius P, Reutter BW, et al. Kinetic analysis of ^{18}F -fluorodihydroxyrotenone as a deposited myocardial flow tracer: comparison to ^{201}Tl . *J Nucl Med*. 2004;45:1950–1959.
9. Yu M, Guaraldi M, Kagan M, et al. Assessment of ^{18}F -labeled mitochondrial complex I inhibitors as PET myocardial perfusion imaging agents in rats, rabbits, and primates. *Eur J Nucl Med Mol Imaging*. 2009;36:63–72.
10. Yu M, Guaraldi M, Mistry M, et al. BMS-747 158-02: a novel PET myocardial perfusion imaging agent. *J Nucl Cardiol*. 2007;14:789–798.
11. Nekolla SG, Saraste A. Novel F-18-labeled PET myocardial perfusion tracers: bench to bedside. *Curr Cardiol Rep*. 2011;13:145–150.
12. Huisman MC, Higuchi T, Reder S, et al. Initial characterization of an ^{18}F -labeled myocardial perfusion tracer. *J Nucl Med*. 2008;49:630–636.
13. Kronauge JF, Chiu ML, Cone JS, et al. Comparison of neutral and cationic myocardial perfusion agents: characteristics of accumulation in cultured cells. *Int J Rad Appl Instrum B*. 1992;19:141–148.
14. Purohit A, Radeke H, Azure M, et al. Synthesis and biological evaluation of pyridazinone analogues as potential cardiac positron emission tomography tracers. *J Med Chem*. 2008;51:2954–2970.
15. Okun JG, Lummen P, Brandt U. Three classes of inhibitors share a common binding domain in mitochondrial complex I (NADH:ubiquinone oxidoreductase). *J Biol Chem*. 1999;274:2625–2630.
16. Mou T, Jing H, Yang W, et al. Preparation and biodistribution of ^{18}F -FP2OP as myocardial perfusion imaging agent for positron emission tomography. *Bioorg Med Chem*. 2010;18:1312–1320.
17. Yang W, Mou T, Peng C, et al. Fluorine-18 labeled galactosyl-neoglycoalbumin for imaging the hepatic asialoglycoprotein receptor. *Bioorg Med Chem*. 2009;17:7510–7516.
18. Zhang X, Cai W, Cao F, et al. ^{18}F -labeled bombesin analogs for targeting GRP receptor-expressing prostate cancer. *J Nucl Med*. 2006;47:492–501.
19. Zhang X, Zhou P, Liu J, et al. Preparation and biodistribution of $^{99\text{m}}\text{Tc}$ -tricarbonyl complex with 4-[(2-methoxyphenyl)piperazin-1-yl]-dithioformate as a potential 5-HT_{1A} receptor imaging agent. *Appl Radiat Isot*. 2007;65:287–292.
20. Mou T, Yang W, Peng C, Zhang X, Ma Y. ^{18}F -labeled 2-methoxyphenylpiperazine derivative as a potential brain positron emission tomography imaging agent. *Appl Radiat Isot*. 2009;67:2013–2018.
21. Yang W, Mou T, Shao G, Wang F, Zhang X, Liu B. Copolymer-based hepatocyte asialoglycoprotein receptor targeting agent for SPECT. *J Nucl Med*. 2011;52:978–985.
22. Tubaro A, Del Favero G, Beltramo D, et al. Acute oral toxicity in mice of a new palytoxin analog: 42-hydroxy-palytoxin. *Toxicon*. 2011;57:755–763.
23. Zhou HJ. *Statistical Methods for Biological Tests*. Beijing, China: People's Medical Publishing House; 1988:1214.